THE JOURNAL OF BIOLOGICAL CHEMISTRY VOL. 288, NO. 16, pp. 11366–11377, April 19, 2013

Loss of Vacuolar H^+-ATPase (V-ATPase) Activity in Yeast Generates an Iron Deprivation Signal That Is Moderated by Induction of the Peroxiredoxin *TSA2*[*][S]

Received for publication, September 13, 2012, and in revised form, February 26, 2013 Published, JBC Papers in Press, March 1, 2013, DOI 10.1074/jbc.M112.419259

Heba I. Diab and Patricia M. Kane[1]

From the Department of Biochemistry and Molecular Biology, SUNY Upstate Medical University, Syracuse, New York 13210

Background: Loss of V-ATPase activity triggers oxidative stress and altered iron homeostasis.
Results: The peroxiredoxin Tsa2p is induced when V-ATPase activity is lost and limits up-regulation of iron intake genes.
Conclusion: Loss of V-ATPase activity induces iron deprivation signals; induction of *TSA2* limits transcriptional signals for iron uptake.
Significance: Defects in organelle pH control disrupt iron and redox homeostasis but activate novel protective mechanisms.

Vacuolar H^+-ATPases (V-ATPases) acidify intracellular organelles and help to regulate overall cellular pH. Yeast *vma* mutants lack V-ATPase activity and allow exploration of connections between cellular pH, iron, and redox homeostasis common to all eukaryotes. A previous microarray study in a *vma* mutant demonstrated up-regulation of multiple iron uptake genes under control of Aft1p (the iron regulon) and only one antioxidant gene, the peroxiredoxin *TSA2* (Milgrom, E., Diab, H., Middleton, F., and Kane, P. M. (2007) Loss of vacuolar proton-translocating ATPase activity in yeast results in chronic oxidative stress. *J. Biol. Chem.* 282, 7125–7136). Fluorescent biosensors placing GFP under transcriptional control of either an Aft1-dependent promoter (P_{FIT2}-GFP) or the *TSA2* promoter (P_{TSA2}-GFP) were constructed to monitor transcriptional signaling. Both biosensors were up-regulated in the *vma2*Δ mutant, and acute V-ATPase inhibition with concanamycin A induced coordinate up-regulation from both promoters. P_{TSA2}-GFP induction was Yap1p-dependent, indicating an oxidative stress signal. Total cell iron measurements indicate that the *vma2*Δ mutant is iron-replete, despite up-regulation of the iron regulon. Acetic acid up-regulated P_{FIT2}-GFP expression in wild-type cells, suggesting that loss of pH control contributes to an iron deficiency signal in the mutant. Iron supplementation significantly decreased P_{FIT2}-GFP expression and, surprisingly, restored P_{TSA2}-GFP to wild-type levels. A *tsa2*Δ mutation induced both nuclear localization of Aft1p and P_{FIT2}-GFP expression. The data suggest a novel function for Tsa2p as a negative regulator of Aft1p-driven transcription, which is induced in V-ATPase mutants to limit transcription of the iron regulon. This represents a new mechanism bridging the antioxidant and iron-regulatory pathways that is intimately linked to pH homeostasis.

Luminal pH is a central feature of organellar identity. In all eukaryotes, intracellular compartmentalization allows segregation of basic biochemical functions to specific membrane-bound organelles. Proteins encounter organelles of increasing acidity as they travel from the cell membrane to mildly acidic early endosomes and highly acidic lysosomes, and this gradient of acidity ensures various functions, such as endocytosis, receptor-ligand dissociation, and activation of lysosomal enzymes (1–4). In higher organisms, aberrant cytosolic and organellar pH results in distinct pathophysiological states, including cardiac failure and neurological diseases (5–8). Although multiple regulatory mechanisms contribute to overall cellular pH, the vacuolar H^+-ATPase is the primary regulator of pH in acidic organelles.

Vacuolar H^+-ATPases (V-ATPases) are ubiquitous, versatile proton pumps that couple ATP hydrolysis to proton translocation across the membranes of vacuoles/lysosomes, endosomes, Golgi apparatus, and secretory vesicles (9, 10) and, in some cells, the plasma membrane (11). They are multisubunit enzymes composed of 14 subunits that are organized into two domains: the peripheral V_1 sector responsible for ATP hydrolysis and the membrane-bound V_0 sector responsible for proton translocation (9, 10). In yeast, deletion of any V-ATPase subunit (*vma* mutant) results in inactivation of the enzyme (9). Although lethal in higher organisms (12, 13), loss of V-ATPase function in yeast is not lethal and results in organelle acidification defects (14, 15). Loss of V-ATPase activity also indirectly compromises functions of the plasma membrane proton pump (Pma1p) (14), alkali cation/H^+ exchangers (16, 17), and buffering systems (18, 19) to induce broad defects in cellular pH homeostasis. Collectively, compromising all of these pH-regulatory mechanisms results in the relative vacuolar alkalinization and cytosolic acidification observed in the *vma* mutants (14,15). Furthermore, loss of pH homeostasis in the mutants appears to drive a number of downstream defects, such as iron misregulation and oxidative stress (20). The yeast *Saccharomyces cerevisiae* provides a tractable system to study cellular responses to abnormal pH homeostasis.

Under oxidizing conditions, several highly conserved redox mechanisms are activated to promote defense against endoge-

* This work was supported, in whole or in part, by National Institutes of Health Grant R01 GM50322 (to P. M. K.).
[S] This article contains supplemental Tables 1 and 2.
[1] To whom correspondence should be addressed: Dept. of Biochemistry and Molecular Biology, SUNY Upstate Medical University, 750 E. Adams St., Syracuse, NY 13210. Tel.: 315-464-8742; Fax: 315-464-8750; E-mail: kanepm@upstate.edu.

nous and exogenous sources of stress. These antioxidant defenses include both proteins that directly detoxify reactive oxygen species and transcriptional responses to build an array of antioxidants capable of response to different types and levels of oxidizing species (21, 22). Previous work has shown that V-ATPase mutants are sensitive to various oxidizing agents and exhibit evidence of endogenous oxidative stress (20, 23). Despite endogenous stress, a microarray analysis revealed that the *vma2*Δ mutant only up-regulated one antioxidant gene, the thioredoxin peroxidase *TSA2* (20). Thioredoxin peroxidases (also known as peroxiredoxins) are highly conserved in all eukaryotes, with well established roles as peroxide detoxifiers (24, 25). In yeast, the housekeeping gene, Tsa1p, and its homolog, the peroxide-induced Tsa2p, cooperate to protect yeast cells from oxidative stress (25, 26). Tsa1p and Tsa2p are 86% identical at the amino acid level, and both are two cysteine peroxiredoxins that have a peroxidatic cysteine at position 47 (27). Overexpression of *TSA2* can partially compensate for loss of *TSA1*, suggesting some overlap in function, and *tsa1*Δ*tsa2*Δ mutants are more sensitive to peroxide than either of the single mutants (25). However, there is additional evidence that these two peroxiredoxins have distinct transcriptional regulation and functions. Tsa2p is induced by peroxide stress, whereas Tsa1p is present at high basal levels (25, 26). Tsa1p has a dual function as housekeeping protein for peroxide detoxification and a chaperone for misfolded proteins (28, 29) but also has multiple regulatory functions, including reducing oxidative stress by binding an iron-regulatory factor, Fra1p (30). Tsa2p also possesses chaperone activity (28) but has not been shown to have a role in iron homeostasis.

In yeast, the uptake and storage of iron is regulated by the transcription factor Aft1p and its paralog Aft2p (31). Under iron-replete conditions, Aft1p is localized predominantly to the cytosol, and upon iron deprivation, it translocates into the nucleus, where it activates the transcription of high affinity iron import and mobilization genes, collectively known as the iron regulon (32, 33). Aft1p does not directly respond to iron levels; instead, its nucleocytoplasmic localization is dependent upon iron-sulfur cluster biogenesis (34). An iron-sulfur cluster bridges iron-regulatory proteins (Fra1p/Fra2p) and glutaredoxins (Grx3p/Grx4p) to form a signaling pathway to Aft1p (30, 35). The absence of this cluster results in constitutive activation of Aft1p regardless of iron levels (36). We have previously shown that transcription of the Aft1p-dependent iron regulon is strongly up-regulated in *vma* mutants (20). In all eukaryotes, V-ATPases provide the acidic environment of endosomes and lysosomes to promote proper iron mobilization and utilization. If regulated incorrectly, iron may react with hydrogen peroxide to catalyze the production of hydroxyl radicals via Fenton reaction, ultimately resulting in indiscriminate cellular damage (37).

In an attempt to understand which of the defects in the *vma* mutant trigger the distinctive induction of *TSA2* and the iron regulon, we generated GFP biosensors under control of the *TSA2* promoter and Aft1p-dependent *FIT2* promoter. Here we show that cytosolic acidification may trigger iron misregulation. Furthermore, although Tsa2p is not known to have a role in iron regulation, we show that its transcription responds to iron levels and that Tsa2p helps to limit Aft1p-driven up-regulation of the iron regulon. Our data suggest that *TSA2* overexpression in the *vma* mutant may be a unique, protective mechanism that bridges the antioxidant and iron homeostasis pathways.

EXPERIMENTAL PROCEDURES

Growth Media, Yeast Strains, and Plasmids—Congenic *aft1*Δ::*kan*^{R}, *aft2*Δ::*kan*^{R}, *tsa1*Δ::*kan*^{R}, *tsa2*Δ::*kan*^{R}, *fra1*Δ::*kan*^{R}, and *yap1*Δ::*kan*^{R} mutations in the BY4741 background (*MATa his3*Δ*1 leu2*Δ*0 met15*Δ*0 ura3*Δ*0*) were purchased from OpenBiosystems. These strains have a complete replacement of the open reading frame with the *kanMX* marker. The BY4742 *vma2*Δ::*nat*^{R} strain (*MATα his3*Δ*1 leu2*Δ*0 lys2*Δ*0 met15*Δ*0 ura3*Δ*0 vma2*Δ::*nat*^{R}) was constructed as described (38). Haploid cells were mated, the resulting diploids were sporulated, and tetrads were dissected to the double mutants. All strains used are listed in supplemental Table 1.

The Aft1p-GFP strain was purchased from Invitrogen and used as the parental strain to generate the deletion mutants. Deletion mutations were introduced either by PCR-mediated amplification of the mutant allele (*tsa2*Δ, *tsa1*Δ, or *vma2*Δ) and transformation into the parental strain or by tetrad dissection (to generate *fra1*Δ Aft1p-GFP). To generate the *fra1*Δ *vma2*Δ Aft1p-GFP strain, *VMA2* was then deleted from this strain by transformation with a *vma2*Δ::*nat*^{R} allele.

To generate pFL-TSA2, the *TSA2* open reading frame plus 1 kb upstream and 0.4 kb downstream flanking sequence was amplified by PCR and inserted into SacII- and ClaI-digested pRS316. Site-directed mutagenesis of Cys-47 to obtain pFL-TSA2^{C47S} was performed by overlap PCR in this plasmid. The mutated inserts were then digested from the pRS316 plasmid and integrated into the *tsa2*Δ::*URA3 vma2*Δ::*nat*^{R} strain harboring the P_{FIT2}-GFP biosensor. Transformants were selected on medium containing 5-fluoroorotic acid as a counterselection for integration of the mutant *TSA2*^{C47S} insert in place of the *tsa2*Δ::*URA3* allele, and the mutation was confirmed by sequencing. N-terminally HA-tagged Tsa2p (HA-Tsa2p) was constructed by overlap PCR mutagenesis of pFL-TSA2 to introduce a single HA epitope immediately after the start codon, using oligonucleotides TSA2-HA-FOR and TSA2-HA-REV. Oligonucleotide sequences are listed in supplemental Table 2.

Yeast cells were grown in YEPD (1% yeast extract, 2% peptone, 2% dextrose) or synthetic complete (SC)[2] medium (0.67% yeast nitrogen base, 2% dextrose, supplemented with the indicated amino acid dropout mix).

GFP Biosensors—To construct the P_{TSA2}-GFP plasmid, a 1-kb upstream region of *TSA2* was PCR-amplified from wild-type genomic DNA using primers EcoRI-P_{TSA2} and P_{TSA2}-GFP (rev). The GFP forward and GFP-BamHI (rev) oligonucleotides were used to PCR-amplify GFP from pTD125. These two pieces were fused using the EcoRI-P_{TSA2} and GFP-BamHI (rev) oligonucleotides. pTD125 was cleaved with EcoRI and BamHI restriction enzymes. The Quick Stick Ligation kit (Bioline) was used to ligate the P_{TSA2}-GFP construct into the pTD125 plas-

[2] The abbreviations used are: SC, synthetic complete; V-ATPase, vacuolar H^+-ATPase.

mid. The resulting construct was transformed into wild-type and *vma2*Δ cells.

GFP was integrated into the *FIT2* open reading frame by standard methods. Oligonucleotides were designed to include 50 bp immediately upstream from the ATG of *FIT2* and 50 bp immediately downstream of the stop sequence of *FIT2* (39). These primers (FIT2-GFP-UP and FIT2-GFP-DOWN) were used to PCR-amplify the GFP cassette out of pFA6a-GFP (S65T)-kanMX6. The resulting fragment was integrated into the *FIT2* ORF by homologous recombination. The *vma2*Δ::*nat*^{R} allele was introduced as described above.

Measurement of Biosensor Fluorescence under Various Conditions—For acute inhibition of the V-ATPase using the concanamycin A (Wako Biochemicals), cells were grown to log phase, pelleted, and washed with YEP (P_{FIT2}-GFP biosensor) or minimal (SC) medium (P_{TSA2}-GFP biosensor, Aft1p-GFP). The pellets were resuspended in 200 μl of YEP or SC medium and incubated without glucose at 30 °C. After 10 min, glucose (50 mM final) and concanamycin A (2 μM final) were added. Fluorescence images were captured after 15, 30, 60, and 90 min of incubation with concanamycin A. Differential interference contrast and GFP fluorescence images were captured on an epifluorescence microscope (Imager-Z1, Zeiss) using a Hamamatsu CCD camera. To quantitate GFP fluorescence, pixel intensity within fluorescent cytosolic areas (dimensions of selection square consistent across all samples) was measured using ImageJ (National Institutes of Health). All graphs illustrate the mean of 20 cells ± S.E.

To mimic the acidic cytosol observed in the *vma* mutants, cells expressing either the GFP biosensors or Aft1p-GFP were grown to log phase and then exposed to 20 mM acetic acid for 30 min. To induce oxidative stress conditions, cells expressing the GFP biosensors were grown to log phase and then exposed to 1 mM hydrogen peroxide for 30 min. To examine the effects of altered iron levels, *vma2*Δ cells containing P_{TSA2}- and P_{FIT2}-GFP biosensors were supplemented with 0.5, 1, or 2 mM ferrous ammonium sulfate for 30 min. Wild-type and *vma2*Δ cells containing biosensors were deprived of iron by the addition of 80 μM bathophenanthroline sulfonate (Sigma) for 4 h.

Protein Analysis and Aconitase Assay—To integrate a triple HA tag at the C terminus of *TSA1* and *TSA2*, oligonucleotides were designed to include 50 bp immediately up- and downstream of the stop codon and used to amplify the 3HA-*HIS3*MX6 cassette from pFA6a-3HA-*HIS3*MX6 (39). The resulting products were confirmed by sequencing and integrated into wild-type cells by homologous recombination. To generate the *vma2*Δ mutant in the tagged strains, *VMA2* was deleted with *URA3* as described above.

To assess protein levels in wild-type and *vma2*Δ strains containing Tsa1–3HA and Tsa2–3HA, cells were grown to log phase, and whole cell lysates were prepared. Samples were separated by SDS-PAGE and transferred to a nitrocellulose membrane, and blots were probed with anti-HA.11 (Covance), monoclonal antibody 8B1 (against Vma1p, the V-ATPase A subunit), and monoclonal antibody 13D11 (against Vma2p, the V-ATPase B subunit) as described previously (40). In order to quantitate the increase in Tsa2-HA fluorescence in the *vma2*Δ mutant, the signals in the Vma1p and HA bands were quantitated using ImageJ (National Institutes of Health), and the ratio of HA/Vma1 signal was calculated.

Immunoprecipitation of Fra1p with HA-Tsa2p was performed as described for coprecipitation with HA-tagged Tsa1p (30) with the following changes. Log phase cultures corresponding to 5.0×10^8 cells of each strain were pelleted by centrifugation, resuspended in 0.5 ml of 25 mM Tris-HCl, pH 7.4, containing 1% Triton X-100 and protease inhibitors, and then lysed by the addition of an equal volume of acid-washed glass beads and five cycles of 1-min vortex mixing followed by 1 min on ice. An additional 0.5 ml of 25 mM Tris-HCl, pH 7.4, was added to dilute the detergent before immunoprecipitation. After centrifugation for 10 min at 15,700 × *g* in a microcentrifuge, the supernatant was collected and incubated overnight with 4 μl of purified mouse monoclonal antibody HA.11 followed by Protein A-Sepharose. Immunoprecipitated protein was separated by SDS-PAGE and immunoblotted with anti-HA.11 (1:1000 dilution) or affinity-purified rabbit anti-Fra1 (1:3000 dilution). Rabbit anti-Fra1 antibody was a generous gift from Jerry Kaplan (University of Utah).

Aconitase activity was measured using an aconitase assay kit from Cayman Chemicals. Yeast lysates were prepared as described by Pierik *et al.* (41) except that glycerol was omitted from the lysis buffer. Initial rates of aconitase activity in wild-type and *vma2*Δ strains were measured at 37 °C using a BioTek Synergy HT plate reader at an absorbance of 340 nm, and the rate in the presence of the aconitase inhibitor oxalomalate was subtracted from the rate in the absence of inhibitor. Each measurement was done in triplicate and averaged, and three independent samples of wild-type and *vma2*Δ lysates were compared.

Measurement of Total Cell Iron Levels—Wild-type and *vma2*Δ cells were grown to log phase in YEPD buffered to pH 5. Approximately 2.5×10^8 cells were harvested and washed in water, and cell pellets digested with 1.25 ml of concentrated, metal ion-free nitric acid for 20–30 min at 55 °C (until the suspension was clear). After a 1:10 dilution of the acid extracts in water, iron levels were measured by inductively coupled plasma atomic emission spectroscopy at the SUNY School of Environmental Science and Forestry.

RESULTS

V-ATPase Mutants Preferentially Express TSA2 and Require AFT1 for Survival—V-ATPase mutants are sensitive to an array of oxidizing agents (20, 23). Despite evidence of endogenous oxidative stress, only one antioxidant gene, *TSA2*, was significantly induced in a previous microarray screen of a *vma2*Δ mutant (20). The pronounced transcriptional up-regulation of *TSA2*, and not its homolog *TSA1* or other antioxidants, suggested that Tsa2p might be important for resistance of *vma* mutants to oxidative stress. To assess if protein levels reflect the preferential transcriptional up-regulation of *TSA2* in the *vma* mutant, a triple hemagglutinin tag was integrated at the C terminus of each peroxiredoxin. Consistent with previous reports (25, 42), we saw significantly higher levels of HA-tagged Tsa1p compared with Tsa2p (Fig. 1*A*). Also, although Tsa1p levels are the same between wild-type and *vma2*Δ, there is 3.3-fold more Tsa2p in the mutant compared with wild-type, confirming

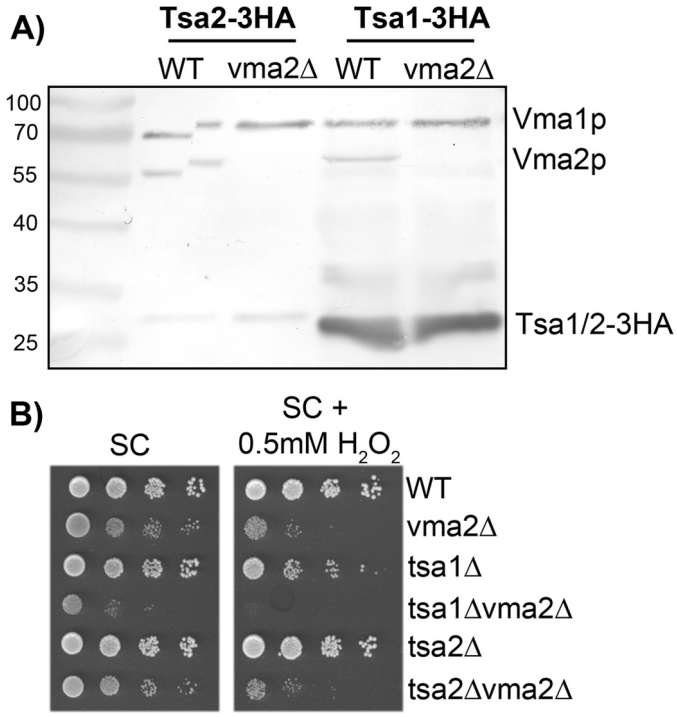

FIGURE 1. **Up-regulation of TSA2 does not protect *vma2*Δ mutants from peroxide.** *A*, wild-type and *vma2*Δ cells containing Tsa1–3HA and Tsa2–3HA were grown to equal densities, and whole cell lysates were prepared as described under "Experimental Procedures." Equal loads for each sample (based on number of cells lysed) were separated by SDS-PAGE followed by Western blot analysis with anti-HA (recognizing Tsa1-HA and Tsa2-HA, as indicated), anti-Vma1p, and anti-Vma2p. Vma2p is missing from the *vma2*Δ samples, as expected, and Vma1p serves as a loading control. (A tear in the gel caused the discontinuity in the *first lane* but does not affect the interpretation of the blot.) Molecular mass standards are shown on the *far left*. *B*, the indicated strains were grown to log phase in liquid culture, adjusted to a density of 0.5×10^7 cells/ml, and then serially 10-fold diluted before pinning onto fully supplemented minimal medium (SC) with and without 0.5 mM H_2O_2. Plates were incubated at 30 °C for 2 days.

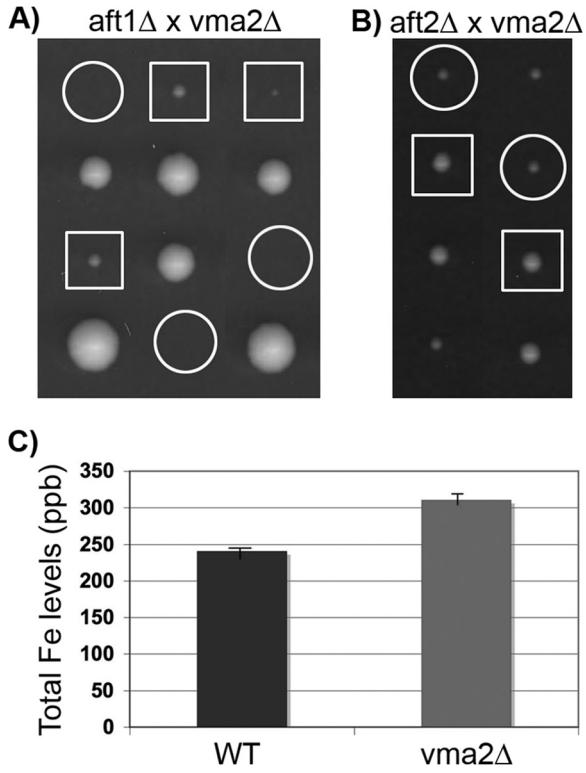

FIGURE 2. ***vma2*Δ mutant requires *AFT1* for survival.** *A* and *B*, the *aft1*Δ*vma2*Δ and *aft2*Δ*vma2*Δ heterozygous diploids were sporulated, tetrads were dissected, and genotypes were determined. *A*, tetrads from dissection of the *aft1*Δ and *vma2*Δ diploid were grown on YEPD, pH 5, for 5 days. The *boxed spores* are *aft1*Δ. The *circles* represent missing spores predicted to have the *aft1*Δ*vma2*Δ genotype. *B*, tetrads from the dissection of the *aft2*Δ and *vma2*Δ diploid were grown on YEPD, pH 5, for 2 days. *Boxed spores* represent *aft2*Δ mutant. *Circles* represent the *aft2*Δ*vma2*Δ double mutant. *C*, total iron levels in wild-type and *vma2*Δ cells were measured by inductively coupled plasma atomic emission spectroscopy, as described under "Experimental Procedures." *Error bars*, S.E.

preferential expression of this protein when V-ATPase activity is lost. If Tsa2p is indeed important for antioxidant defense in *vma2*Δ mutants, then its loss might increase sensitivity to peroxide. We generated haploid double mutants by crossing *vma2*Δ to the *tsa1*Δ or *tsa2*Δ mutants. Growth assays were performed to assess the ability of each peroxiredoxin to protect yeast cells from exogenous hydrogen peroxide (Fig. 1*B*). The growth of wild-type *versus tsa2*Δ and *vma2*Δ *versus tsa2*Δ*vma2*Δ cells was the same, suggesting there was no additional peroxide sensitivity in the *tsa2*Δ mutants. However, *tsa1*Δ was more sensitive to peroxide than wild type, and the *tsa1*Δ*vma2*Δ mutant was much more sensitive than the strain containing *vma2*Δ alone. This suggests that *TSA1* is more important than *TSA2* for defense against exogenous peroxide stress both in wild-type and *vma2*Δ cells. Up-regulation of *TSA2* may serve a role other than peroxide detoxification in the *vma2*Δ mutant.

The acidification of vacuoles, the Golgi apparatus, and endosomes by V-ATPases is crucial for proper iron uptake and utilization (1, 43). Loss of V-ATPase function results in a striking induction of iron import and mobilization genes (the "iron regulon") controlled by the transcription factor Aft1p (20). Aft1p induces transcription of the iron regulon upon iron deprivation, suggesting that the *vma2*Δ mutant is starved of this metal. If up-regulation of the iron regulon is required for survival of the mutant, then loss of *AFT1* will be lethal in combination with a *vma* mutation. As shown in Fig. 2, *vma2*Δ was crossed to *aft1*Δ or *aft2*Δ haploid mutants, and double mutants were generated. The *aft1*Δ and *vma2*Δ heterozygous diploid did not yield four-spore tetrads even after 5 days of growth on rich media, and genotype analysis of the remaining spores indicated that *aft1*Δ*vma2*Δ spores were missing (Fig. 2*A*). In contrast, deleting the *AFT1* paralog, *AFT2*, does not result in lethality in combination with the *vma* mutation because all of the spores grew after 2 days of growth (Fig. 2*B*). This suggests that *AFT1* is necessary for survival of the *vma2*Δ mutant.

In order to directly assess iron status of the *vma2*Δ mutant, we measured total cell iron levels with inductively coupled plasma atomic emission spectroscopy. Interestingly, the *vma2*Δ mutant had levels of total iron comparable with wild type (Fig. 2*C*). Overall, these data suggest an iron signaling or distribution defect; despite sufficient cellular total iron levels, the iron regulon is highly up-regulated, suggesting that the *vma* mutant continually senses iron deprivation.

Communication of iron levels to Aft1p requires iron-sulfur cluster-containing proteins; defects in biosynthesis of iron sulfur clusters or conditions that damage these clusters can induce

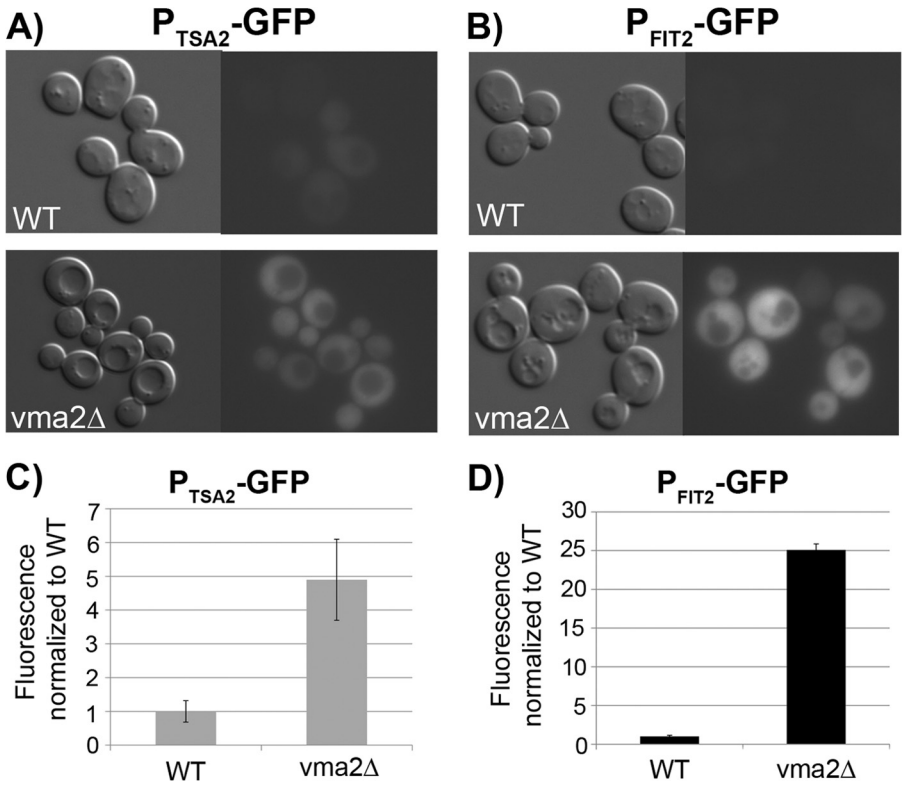

FIGURE 3. **P_{FIT2}-GFP and P_{TSA2}-GFP biosensors provide a measure of *FIT2* and *TSA2* up-regulation in *vma2*Δ.** *A*, wild-type (*top*) and *vma2*Δ cells (*bottom*) containing P_{TSA2}-GFP were grown in SC-uracil medium. *B*, wild-type (*top*) and *vma2*Δ cells (*bottom*) containing P_{FIT2}-GFP were grown in YEPD buffered to pH 5. In both *A* and *B*, cells are viewed under Nomarski (*left* of each set) and GFP fluorescence (*right*) optics. A 500-ms exposure time was used to capture fluorescence images. *C* and *D*, cytosolic fluorescence intensities of 20 cells for each sample were quantitated using ImageJ (National Institutes of Health), as described under "Experimental Procedures," and normalized to the fluorescence of wild-type cells containing each sensor. Normalized mean fluorescence is shown, with *error bars* representing S.E.

the iron regulon (34, 44–47). In order to test the hypothesis that iron-sulfur cluster biosynthesis or stability might be affected in the *vma* mutants, we measured the activity of a representative iron-sulfur cluster-dependent enzyme, aconitase (41). In three independent experiments, aconitase activity in the *vma2*Δ mutant was 40.9 ± 12.5% (mean ± S.E., $n = 3$) the activity in wild-type cells. These results suggest that the *vma2*Δ mutant may have an iron-sulfur cluster defect that contributes to up-regulation of the iron regulon in cells.

Acute Inhibition of V-ATPase Activity Induces FIT2 and TSA2 Expression—Up-regulation of *TSA2* and the iron regulon are "transcriptional trademarks" of the *vma2*Δ mutant. To better understand the distinctive expression pattern observed in the V-ATPase mutant, we developed genetic tools that allow transcriptional changes in *TSA2* and the iron regulon (represented by the functionally redundant iron import gene *FIT2*) to be visually monitored as cells are manipulated. Constructs driving GFP expression from the *TSA2* and *FIT2* promoters were designed to provide a fluorescent output of transcriptional changes. A plasmid-borne copy of a P_{TSA2}-GFP biosensor (*TSA2* promoter driving GFP production) was transformed into wild-type and *vma2*Δ cells. The P_{FIT2}-GFP biosensor (*FIT2* promoter driving GFP production) was integrated at the *FIT2* genomic locus in wild-type and *vma2*Δ cells. There is very little fluorescence from P_{TSA2}-GFP sensor in wild-type cells (Fig. 3*A*) and none detected from the P_{FIT2}-GFP sensor (Fig. 3*B*). However, there is clear GFP fluorescence driven from both promoters in the *vma2*Δ mutant. These transcriptional changes are consistent with our microarray screen, confirming that the biosensors are functional and consistent with transcriptional responses determined by other methods (20).

Iron misregulation and oxidative stress are clearly linked. High levels of reactive oxygen species, such as hydrogen peroxide, can react with iron via the Fenton reaction to generate hydroxyl radicals, that have the capacity to induce indiscriminate cellular damage, including but not limited to iron-sulfur clusters (37). Also, Irazusta *et al.* (48) showed that iron overload can trigger oxidative stress by selective protein carbonylation and that targets of iron overload-induced oxidation can be antioxidants themselves. We hypothesized that the *vma* mutants might be subject to combined effects of compromised iron homeostasis and endogenous oxidative stress; however, it is unclear which pathway is first compromised by loss of V-ATPase activity. In addition, the pleiotropic defects of the *vma* mutants make it very difficult to define the original source of these defects. Therefore, we sought to pinpoint the root of the defects in iron and oxidative metabolism by acutely inhibiting the V-ATPase and by mimicking individual defects seen in the *vma* mutants and then examining their effects on the transcriptional biosensors.

To acutely inhibit V-ATPase activity, wild-type cells containing the biosensors were incubated with the V-ATPase-specific inhibitor, concanamycin A, at concentrations shown previously to inhibit vacuolar acidification (14). GFP fluorescence was

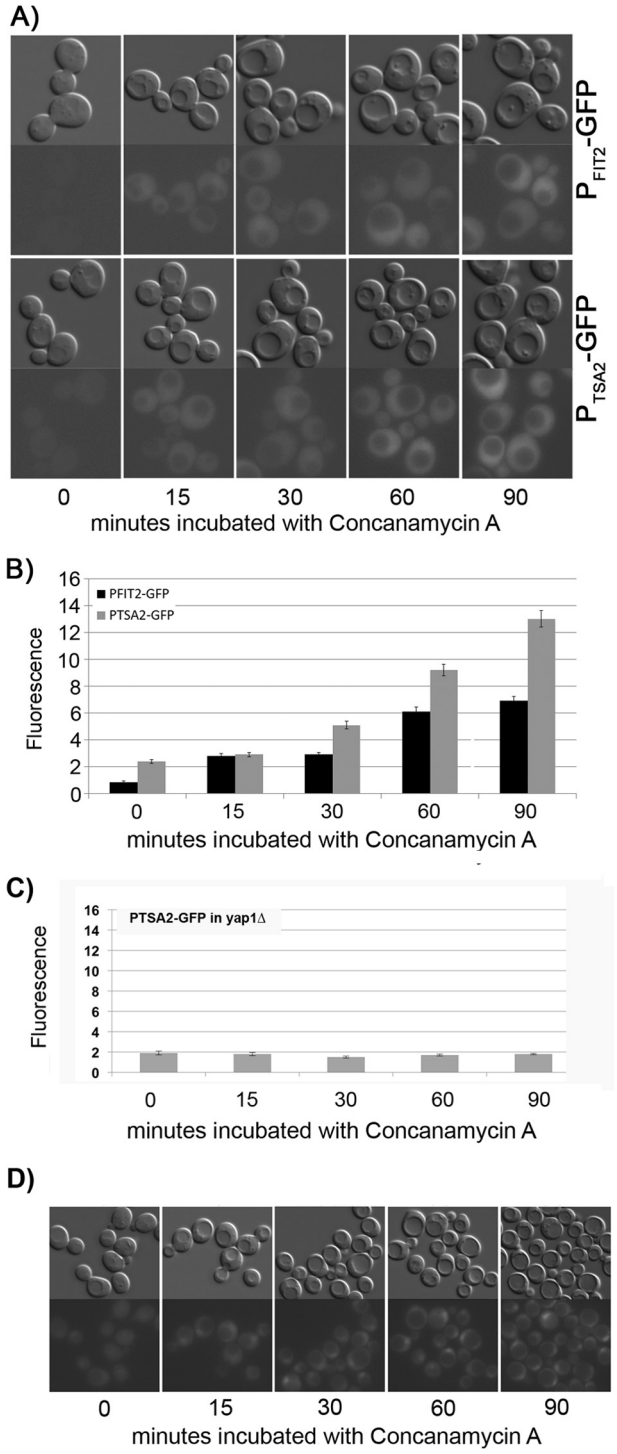

FIGURE 4. ***TSA2* and *FIT2* responses to acute loss of V-ATPase activity are fast and synchronized.** *A*, 2 μM concanamycin A was added to wild-type cells containing P_{TSA2}-GFP and P_{FIT2}-GFP to inhibit V-ATPase activity. GFP fluorescence from each sensor was monitored 15, 30, 60, and 90 min after concanamycin addition. *B*, GFP fluorescence intensities of 20 cells for each sample were quantitated using ImageJ and are shown as mean fluorescence intensity ± S.E. (*error bars*). *C*, the P_{TSA2}-GFP biosensor was introduced into a *yap1*Δ cell line, the cells were treated with concanamycin A, and fluorescence intensity was quantitated as in *A* and *B*. *D*, wild-type cells containing Aft1p-GFP cells were exposed to concanamycin A as in *A* and *B*. Fluorescence images were captured through a 6-s exposure time.

TABLE 1

Effects of pH and H_2O_2 on P_{FIT2}- and P_{TSA2}-GFP expression

Wild-type (WT) cells containing P_{FIT2}- and P_{TSA2}-GFP were exposed to 1 mM H_2O_2 or 20 m M acetic acid to mimic endogenous oxidative stress and cytosolic acidification observed in *vma2*Δ. To assess if iron regulon and *TSA2* transcription can be modulated by partially normalizing cytosolic pH of *vma* mutants, *vma2*Δ cells containing P_{FIT2}- and P_{TSA2}-GFP were incubated in at pH 7. Images were captured and quantitated as in Fig. 3. Mean fluorescence of 20 cells ± S.E. is listed.

	P_{FIT2}-GFP	1mM H_2O_2	20mM Acetic Acid	pH 7
WT	1	1.4 ± 0.2	5 ± 0.3	--
*vma2*Δ	25 ± 0.8	--	--	6.6 ± 0.5

	P_{TSA2}-GFP	1mM H_2O_2	20mM Acetic Acid	pH 7
WT	1	1.3 ± 0.5	1.3 ± 0.5	--
*vma2*Δ	4.9 ± 1.2	--	--	2.9 ± 0.7

assessed by fluorescence microscopy after 15, 30, 60, and 90 min of concanamycin A incubation. Overall, the transcriptional responses from the P_{FIT2}-GFP and P_{TSA2}-GFP biosensors were rapid and relatively synchronized (Fig. 4*A*). P_{FIT2}-GFP was detected within 15 min of V-ATPase inhibition, as seen by a 2-fold change in fluorescence that progressively increased with longer incubation times, resulting in an 8.2-fold increase in fluorescence after 90 min in concanamycin A (Fig. 4*B*). Although induction of P_{TSA2}-GFP was slightly delayed compared with P_{FIT2}-GFP, it too gradually increased with longer concanamycin A incubation times, reaching a 5.4-fold increase in fluorescence after 90 min (Fig. 4*B*). The parallel rise in GFP fluorescence from both of the promoters suggests that the oxidative stress and iron regulation pathways may be more intertwined in the *vma2*Δ mutant than previously appreciated. We also compared the level of induction of the two biosensors in response to concanamycin A to the fluorescence levels in the *vma2*Δ mutant relative to wild type. The 5.4-fold induction of P_{TSA2}-GFP was comparable with the 4.9-fold higher level of GFP fluorescence in the *vma2*Δ mutant compared with wild-type cells (Table 1). The 8.2-fold higher P_{FIT2}-GFP fluorescence after concanamycin is 32% of the 25-fold increase seen in the *vma2*Δ mutant (Table 1).

The signal inducing *TSA2* transcription in the *vma2*Δ mutant is not known, but the P_{TSA2}-GFP biosensor provides a mechanism for addressing this question. The *TSA2* promoter contains a number of potential sites for stress-activated transcription factors (49), including Yap1p, a redox-sensitive regulator of the transcriptional response to oxidative stress (50). A *yap1*Δ mutant was transformed with the P_{TSA2}-GFP biosensor and then treated with concanamycin A. As shown in Fig. 4*C*, the up-regulation of the P_{TSA2}-GFP biosensor was completely absent in the *yap1*Δ strain, suggesting that Yap1p is essential for the up-regulation of *TSA2* in response to loss of V-ATPase activity.

Transcription of the iron regulon is induced by recruitment of Aft1p to the nucleus in response to iron deprivation signals (33). To verify that the rise of P_{FIT2}-GFP fluorescence coincided with nuclear localization of Aft1p, we exposed wild-type cells containing GFP-tagged Aft1p (Aft1p-GFP) to concanamycin A under the same conditions to look at expression of the P_{FIT2}-GFP biosensor. Aft1p-GFP indeed translocated from the cytosol to the nucleus after 15 min, and the concentration in the nucleus increased with longer incubation times (Fig. 4*D*). The

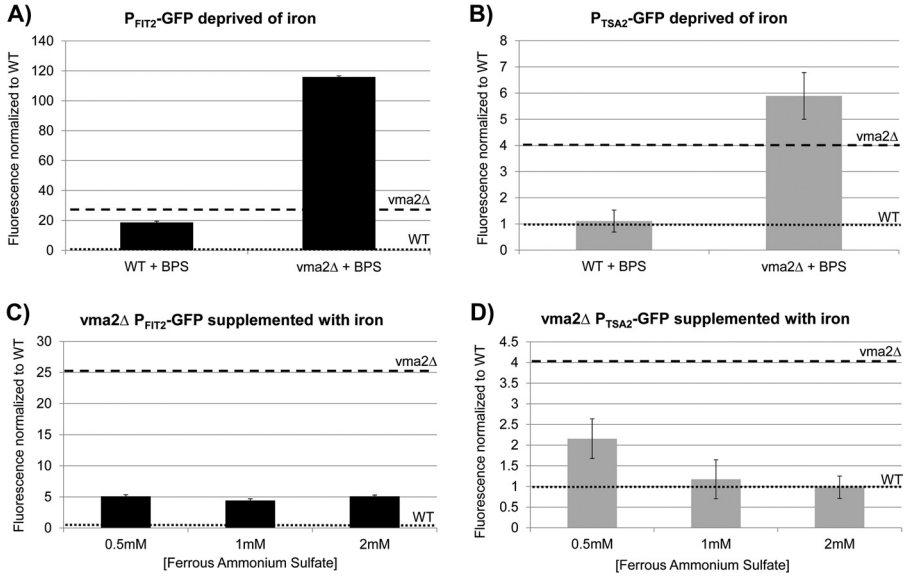

FIGURE 5. **Manipulation of extracellular iron levels changes both P_{FIT2}-GFP and P_{TSA2}-GFP expression in *vma2*Δ cells.** *A* and *B*, wild-type and *vma2*Δ cells containing P_{FIT2}-GFP (*A*) or P_{TSA2}-GFP (*B*) were grown to log phase and incubated with the iron chelator bathophenanthroline sulfonate (*BPS*) at 80 μM for 4 h. Levels of cellular fluorescence in untreated wild-type (*dotted line*) and *vma2*Δ cells (*dashed line*) from Fig. 3 are shown as *horizontal lines*, and all values are normalized to fluorescence of the untreated wild-type strain. *C* and *D*, *vma2*Δ cells with P_{FIT2}- or P_{TSA2}-GFP were supplemented with 0.5, 1, and 2 mM ferrous ammonium sulfate for 30 min. Normalized fluorescence is shown as in *A* and *B*. For all *panels*, images were captured and quantitated as in Fig. 4, *A* and *B*. The mean fluorescence of 20 cells is shown, with *error bars* representing S.E.

rapid P_{FIT2}-GFP expression and Aft1p-GFP nuclear localization suggest that the *vma* mutant does indeed sense iron deprivation and, as a result, induce transcription of the iron regulon.

Cytosolic Acidification Triggers Iron Regulon Expression—Loss of pH homeostasis in the *vma2*Δ mutants has several potential downstream consequences that could contribute to the transcriptional changes we observe. To assess if peroxide stress activates transcription of either biosensor, we exposed wild-type cells to an exogenous oxidant, 1 mM H_2O_2. After 30 min, there was no increase in GFP expression from P_{TSA2}-GFP or P_{FIT2}-GFP (Table 1), suggesting that this exogenous oxidative stress, at least at relatively low levels, does not trigger activation of *TSA2* or the iron regulon in *vma2*Δ mutants. Second, V-ATPase mutants have a more acidic cytosol than wild-type cells (14). An acidic environment not only promotes iron bioavailability (51) but can also damage iron-sulfur clusters (47). Both of these can perturb iron homeostasis and promote oxidative stress. To begin to assess if cytosolic acidification compromises iron regulation and triggers transcription of *FIT2* or *TSA2*, we exposed wild-type cells containing both biosensors to acetic acid as a cell-permeant weak acid. As shown in Table 1, after 30 min of incubation with 20 mM acetic acid, P_{TSA2}-GFP expression was not affected, but interestingly, there was a 4-fold increase in P_{FIT2}-GFP expression in the acid-treated cells. This suggests that the acidic cytosol in *vma2*Δ may contribute to induction of the iron regulon but not to *TSA2* transcription. Last, although V-ATPase mutants grow poorly at elevated pH, incubation of the mutants at alkaline pH for a few h results in a less acidic cytosol (14). *vma2*Δ cells expressing the biomarkers were grown in rich medium buffered to pH 5 and then shifted to pH 7 for 3 h. There was a 72% reduction in P_{FIT2}-GFP and a 40% reduction in P_{TSA2}-GFP signal. Together, these data suggest that the acidic cytosol of *vma* mutants may be a major contributor to transcriptional activation of the iron regulon and, to a lesser extent, *TSA2*.

TSA2 Has an Iron-regulatory Role—Although total iron levels are comparable with wild type in the *vma2*Δ mutant (Fig. 2*C*), there is an induction in Aft1p-regulated transcription, suggesting that this mutant continues to sense iron starvation. We hypothesized that if defects in iron signaling resulted in localized iron excess, iron chelation might normalize iron signaling. We incubated wild-type and *vma2*Δ cells with a 80 μM concentration of the iron chelator, bathophenanthroline sulfonate, for 4 h and then measured GFP fluorescence. As shown in Fig. 5*A*, there is increased GFP expression from the *FIT2* promoter, suggesting that decreasing extracellular iron availability further promotes induction of the iron regulon by the *vma* mutant. Interestingly, a similar trend is seen for P_{TSA2}-GFP (Fig. 5*B*).

However, if *vma* mutants actually are signaling iron deprivation despite nearly normal total cellular levels, then supplementing this metal might decrease biosensor transcription. *vma2*Δ cells were supplemented with 0.5–2 mM concentrations of ferrous ammonium sulfate for 30 min, and then GFP fluorescence from the biosensors was measured. Indeed, P_{FIT2}-GFP transcription significantly decreased at all concentrations (0.5, 1, and 2 mM) of supplemented iron (Fig. 5*C*) but was not restored to wild-type levels, possibly resulting from the inability of the *vma* mutant to properly import, utilize, or store iron (52, 53). Interestingly, expression of the P_{TSA2}-GFP construct was reduced to wild-type levels when the *vma2*Δ cells were supplemented with 2 mM iron (Fig. 5*D*). This suppression of *TSA2* transcription upon iron addition reveals a potentially new role for this peroxiredoxin. Its up-regulation in the *vma* mutant may be a unique response to imbalances in iron homeostasis.

Li *et al.* (30) showed that in cells with defective mitochondrial-vacuolar iron signaling, Tsa1p can physically bind a negative regulator of Aft1p, Fra1p, and form a complex that minimizes

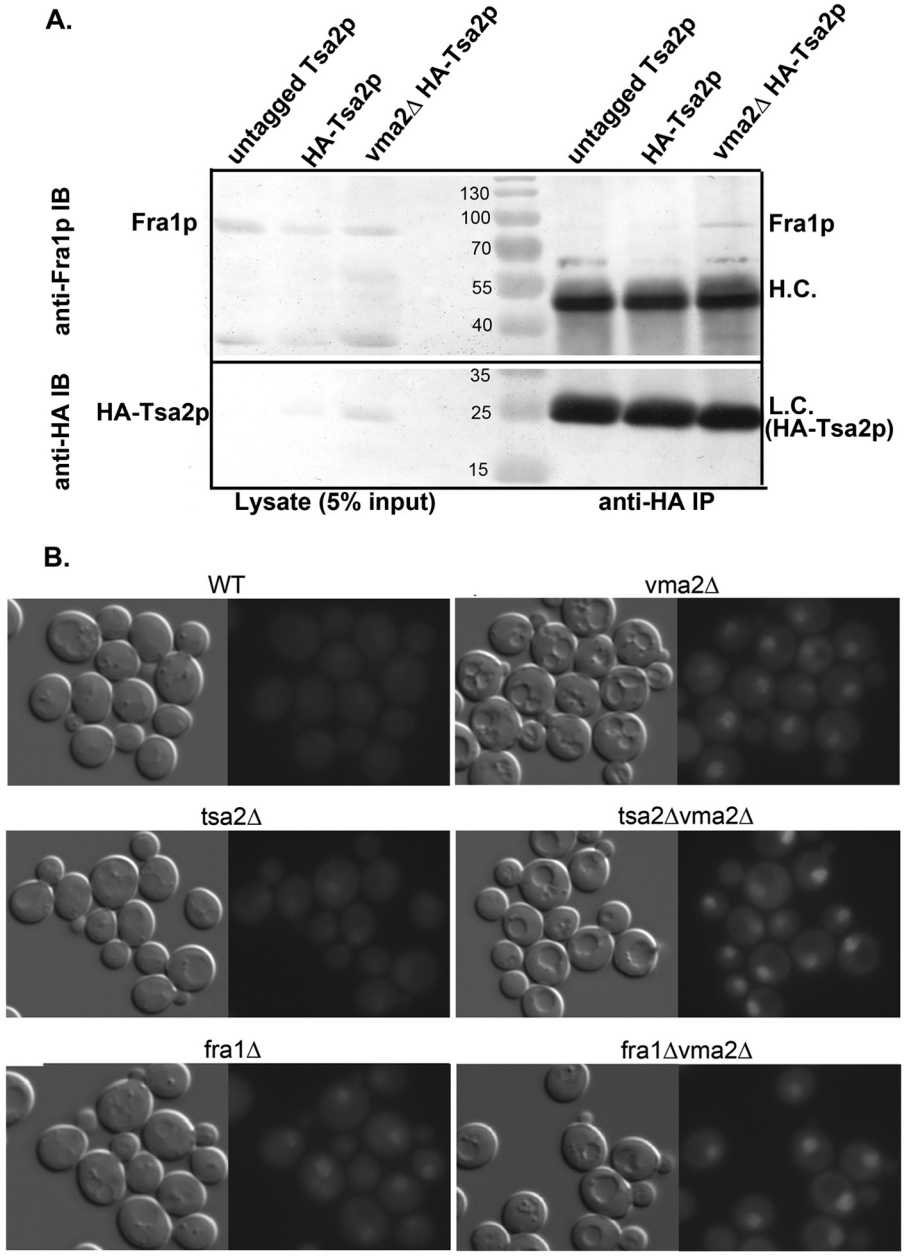

FIGURE 6. **Tsa2p interacts with Fra1p and may limit nuclear localization of Aft1p in *vma2*Δ mutants.** *A*, *tsa2*Δ and *tsa2*Δ*vma2*Δ mutants were transformed with HA-Tsa2p on a plasmid to generate HA-Tsa2p and *vma2*Δ HA-Tsa2p strains, respectively. Wild-type cells served as an untagged Tsa2p control. Lysates were prepared from all strains (equivalent cell numbers for each strain), and anti-HA immunoprecipitations were performed as described under "Experimental Procedures." Equal volumes of lysates from the three strains (corresponding to 5% of the input into the immunoprecipitations) and the anti-HA immunoprecipitates were separated by SDS-PAGE and transferred to nitrocellulose. The blot was cut at the 35 kDa molecular mass marker, the top of the blot was probed with rabbit anti-Fra1p, and the bottom of the blot was probed with mouse anti-HA. Predicted positions of Fra1p and HA-Tsa2p are shown. *H.C.* and *L.C.*, heavy and light chains of the anti-HA antibody used for immunoprecipitation. (The light chain obscures the HA-Tsa2p in the immunoprecipitates.) *B*, wild-type or the indicated mutant cells were visualized under Nomarski optics (*left side* of each set). Fluorescence images (*right side* of each set) of Aft1p-GFP were captured as described using a 6-s exposure time. *IB*, immunoblot; *IP*, immunoprecipitation.

oxidative stress. The Fra1p/Tsa1p interaction has been proposed to serve as a bridge between the oxidative and iron defense mechanisms. In order to test whether Tsa2p can also bind to Fra1p, we introduced a plasmid expressing HA-tagged Tsa2p under its own promoter into *tsa2*Δ (HA-Tsa2p) and *vma2*Δ*tsa2*Δ (*vma2*Δ HA-Tsa2p) cells. As shown in the lysate samples in Fig. 6*A*, HA-Tsa2p was expressed at higher levels in the *vma2*Δ mutant background, as expected, and Fra1p was present in both strains containing HA-Tsa2p and the untagged Tsa2p control. Immunoprecipitation with anti-HA antibody resulted in co-precipitation of Fra1p from the *vma2*Δ HA-Tsa2p sample, with no detectable Fra1p in the immunoprecipitates from the HA-Tsa2p and untagged control. Given the very low levels of HA-Tsa2p in lysates when wild-type *VMA2* is present, we cannot conclude that Fra1p cannot interact with Tsa2p in this strain. However, the results in Fig. 5*A* do indicate that Fra1p does bind to HA-Tsa2p expressed in the *vma2*Δ background.

The Fra1p/Tsa1p interaction negatively regulates Aft1p-dependent transcription (30). To test whether Tsa2p also plays a

TABLE 2

Increased Aft1p-mediated transcription in *fra1*Δ*vma2*Δ, *tsa2*Δ*vma2*Δ, and *tsa1*Δ*vma2*Δ mutants

All cells were grown in SC medium, and P_{FIT2}-GFP expression was measured in *tsa1*Δ, *tsa2*Δ, *fra1*Δ, and *vma2*Δ single and double mutant strains (described under "Experimental Procedures"). Images were captured and quantitated as in Fig. 3. Normalized mean fluorescence of 20 cells ± S.E. is listed.

Strain	P_{FIT2}-GFP fluorescence normalized to WT
WT	1 ± 0.2
*vma2*Δ	35 ± 0.8
*fra1*Δ	8.2 ± 0.3
*tsa1*Δ	0.9 ± 0.1
*tsa2*Δ	4 ± 0.3
*fra1*Δ*vma2*Δ	82 ± 2
*tsa1*Δ*vma2*Δ	77 ± 3
*tsa2*Δ*vma2*Δ	72 ± 2.5
*tsa2*Δ*vma2*Δ/*TSA2*	32 ± 1
*tsa2*Δ*vma2*Δ/*TSA2*^{C47S}	38 ± 0.9

role in regulating transcription of the iron regulon, we introduced the P_{FIT2}-GFP biosensor into the *tsa1*Δ, *tsa2*Δ, and *fra1*Δ single mutants as well as the double deletions with *vma2*Δ and measured GFP fluorescence. As reported previously (35), Aft1p-driven transcription is up-regulated in the *fra1*Δ mutant, as shown by 8-fold induction of P_{FIT2}-GFP (Table 2). Interestingly, the *tsa1*Δ mutation does not induce P_{FIT2}-GFP transcription relative to wild type, but there is a 4-fold induction of GFP expression in the *tsa2*Δ mutant, suggesting that even the very low levels of Tsa2p present in wild-type cells may temper Aft1p-mediated transcriptional activity. Furthermore, all of the double mutants exhibited a 70–80-fold induction compared with wild-type cells, suggesting that Fra1p, Tsa2p, and Tsa1p are acting as negative regulators of Aft1p-driven transcription in the *vma2*Δ mutant.

We assessed nuclear translocation of Aft1p-GFP in several of these strains to confirm that the induction of P_{FIT2}-GFP was accompanied by translocation of Aft1p to the nucleus, and the results are shown in Fig. 6*B*. As expected, in the *fra1*Δ mutant, Aft1p-GFP is localized to the nucleus, and levels in the nucleus increase in the *fra1*Δ*vma2*Δ mutant. This same trend is seen in *tsa2*Δ and *tsa2*Δ*vma2*Δ, suggesting that both Fra1p and Tsa2p help to retain Aft1p in the cytosol and thus limit transcription of the iron regulon. Overall, these data suggest that Tsa2p can exert a negative feedback on Aft1p-driven transcription by helping to retain Aft1p in the cytosol. Up-regulation of *TSA2* in the *vma* mutant helps to limit transcription of the iron regulon by limiting recruitment of Aft1p to the nucleus, and, based on the results in Fig. 6*A*, this role may be mediated, at least in part, through interaction of the induced Tsa2p with Fra1p. These results point toward a novel role for Tsa2p and expand the bridging mechanism between antioxidant and iron-regulatory pathways first proposed by Li *et al.* (30).

Peroxiredoxins have been shown to have both redox and chaperone activities (54). To determine if the redox activity of Tsa2p is required to regulate induction of the iron regulon, a mutation substituting a serine residue for the critical cysteine at position 47 (C47S) was integrated into the *TSA2* open reading frame. Mutating the corresponding cysteine in Tsa1p fully disrupts peroxidase activity (55). Replacing the *tsa2*Δ mutant allele in a *tsa2*Δ*vma2*Δ double mutant with a wild-type *TSA2* allele restored the GFP fluorescence of the P_{FIT2}-GFP biosensor to the level of the *vma2*Δ mutant. Significantly, replacing the *tsa2*Δ allele with a *TSA2*^{C47S} mutant allele displays a similar trend (Table 2). This suggested that the peroxidase activity is not required for the iron-regulatory role of Tsa2p.

DISCUSSION

V-ATPase Activity Is Crucial for Proper Iron and Redox Regulation—V-ATPases coordinate with other pH-regulating mechanisms to establish and maintain cytosolic and organelle pH. Chronic or acute inhibition of V-ATPase activity compromises pH homeostasis on many levels (14, 16, 18, 19). *vma* mutants are slow to respond to cytosolic acidification and never reach the final cytosolic pH of wild-type cells (15). Our results suggest that prolonged cytosolic acidification contributes to many of the transcriptional responses we observe in the *vma2*Δ mutant. Although cytosolic pH changes are achieved through multiple mechanisms, the major determinant of vacuolar pH is the V-ATPase, and vacuolar acidification is almost completely absent in *vma* mutants (14). Importantly, the acidic environment of the vacuole is required to sequester and detoxify metals such as iron and to minimize the generation of reactive oxygen species (37, 43).

There is substantial evidence that iron availability, uptake, and storage are directly dependent upon extracellular, cytosolic, and organelle pH (53, 56). Iron becomes a limiting factor for growth of yeast cells at alkaline extracellular pH (56), and *vma* mutants were shown previously to be sensitive to low iron levels (53). Here we show that both chronic loss of pH homeostasis in *vma* mutants (Fig. 3) and acute inhibition of V-ATPase activity by concanamycin A result in rapid induction of Aft1p-mediated transcription (Fig. 4). Together, these data suggest that the loss of V-ATPase activity can trigger an iron deprivation signal that may ultimately perturb iron distribution or regulation.

Previous work has shown that V-ATPase mutants are sensitive to an array of oxidizing species (20, 23). Interestingly, the only antioxidant we found to be transcriptionally up-regulated in our microarray studies was *TSA2* (20). Because Yap1p is a redox-sensitive transcription factor that might be expected to activate many antioxidant genes (50), we initially doubted that it could account for up-regulation of *TSA2* in response to loss of V-ATPase activity, although there are established Yap1p binding sites in the *TSA2* promoter (49). However, up-regulation of the P_{TSA2}-GFP biosensor in response to acute inhibition of V-ATPase activity is entirely eliminated in a *yap1*Δ mutant (Fig. 4*C*), suggesting that Yap1p is indeed required for *TSA2* up-regulation. Further work will be necessary to understand the apparent specificity of this response for *TSA2*, but the results suggest that an acute loss of V-ATPase activity rapidly generates an oxidative stress signal that is relayed to Yap1p, resulting in *TSA2* up-regulation. Interestingly, the results in Fig. 1 indicate that loss of *TSA2* induction does not make *vma2*Δ mutants more sensitive to exogenous oxidative stress. Instead, our results suggest that the ultimate consequence of Yap1-induced up-regulation of *TSA2* may be altered iron regulation.

Defects in Iron Regulation in the vma Mutant—*vma2*Δ mutants have impaired iron uptake through the plasma membrane high affinity iron import complex, Fet3p-Ftr1p, as a result of poor maturation of this complex (53, 57). However, we found that the *vma2*Δ mutant had nearly normal total cell iron

levels when grown under acidic conditions (YEPD, pH 5; Fig. 2*C*), perhaps because Fet3p can still localize to the plasma membrane in the V-ATPase mutant (53) and be activated in the presence of copper at low extracellular pH. Furthermore, even if the Fet3p-Ftr1p complex is poorly functional, other iron uptake mechanisms are also up-regulated and can probably compensate (31, 58). Previous work has shown that mutating the Fra1p/Fra2p-Grx3p/Grx4p complex results in defective sensing and signaling of iron levels and subsequent iron-independent nuclear localization of Aft1p (35). Similarly, high affinity iron import continues to be up-regulated in the *vma* mutant despite apparently sufficient iron levels (Figs. 2 and 3), suggesting defects in iron sensing and signaling to Aft1p.

This work suggests several possible mechanisms for these signaling defects. First, iron signaling is dependent on iron-sulfur cluster biosynthesis (34, 45), and reduced levels of the iron-sulfur cluster-dependent enzyme aconitase in the *vma2*Δ mutant suggest that the biosynthesis or stability of these clusters may be compromised in the mutant. Second, it is possible that the *vma* mutant senses that it is deprived of iron because of its inability to store and detoxify this metal. When *vma2*Δ cells were supplemented with iron, transcriptional signaling from the iron regulon was dramatically reduced but, interestingly, not to wild-type levels (Fig. 5*C*). However, it was surprising to see transcription of an Aft1p target induced within 15 min of V-ATPase inhibition with concanamycin A (Fig. 4), particularly because the vacuoles might be expected to retain sufficient iron stores under these conditions. Mutants with defective vacuolar acidification have lower levels of iron-binding polyphosphates in the vacuole, which ultimately compromises iron storage (18, 52, 59), but we did not expect to see an immediate collapse of these stores.

Vacuolar iron storage may be compromised by high vacuolar pH, but the prolonged cytosolic acidification observed in V-ATPase mutants (15) may also create defective iron homeostasis. Interestingly, previous work in bacteria revealed an induction of iron starvation response at acidic pH (51). Indeed, we observed that inducing cytosolic acidification with a permeant weak acid in wild-type cells increased Aft1p-mediated transcription. Partially normalizing cytosolic pH by incubating the *vma* mutant in an alkaline environment also reduced Aft1p-mediated transcription (Table 1). Both of these results were surprising. Because iron is more soluble at an acidic pH, iron bioavailability would be expected to increase at low pH, potentially suppressing the signal for Aft1p-mediated transcription (56). Furthermore, poor growth of *vma* mutants at alkaline pH has been attributed in part to poor iron bioavailability (56), which would be expected to stimulate iron deprivation signaling. However, it has been shown that intracellular acidification can catalyze oxidation (51) or protonation (47) of iron-sulfur clusters, resulting in cluster instability and, ultimately, compromised iron signaling. Therefore, it is also possible that the fundamental defect in iron signaling in the *vma* mutants arises from poor pH homeostasis or, more specifically, from cytosolic acidification. Consistent with a complex relationship between iron signaling, Aft1p activation, and loss of V-ATPase activity, we observed synthetic lethality between *aft1*Δ and *vma2*Δ mutations (Fig. 2), but this lethality was not suppressed by dissecting and germinating spores on medium containing 1 mM ferrous ammonium sulfate (data not shown).

TSA2 Has a Regulatory Role in Iron Homeostasis—The sensitivity of the *vma* mutants to exogenous oxidative stress, combined with evidence of chronic oxidative damage, suggested saturation of antioxidant systems and/or a failure to appropriately induce these systems in response to an oxidative challenge (20, 23). In addition, loss of iron regulation may tax antioxidant systems or directly catalyze damage to these systems. Up-regulation of *TSA2* in the *vma2*Δ mutant, coupled with the unique response of P_{TSA2}-GFP to iron levels, indicates a new mechanism for cross-talk between the redox and iron homeostasis systems that may become particularly important when V-ATPase activity is compromised. After 30 min of V-ATPase inhibition with concanamycin A, there appears to be an induction of P_{TSA2}-GFP and stabilization of Aft1p-mediated transcription of P_{FIT2}-GFP, which was repeated again at 90 min of inhibition (Fig. 4). This could suggest that Yap1p induces *TSA2* expression when Aft1p-driven transcription, and possibly iron uptake, reaches a certain threshold, and then Tsa2p helps to limit Aft1p activity. The Fra1p/Tsa2p interaction shown in Fig. 6*A* and the comparable increases in P_{FIT2}-GFP expression in *vma2*Δ*fra1*Δ and *vma2*Δ*tsa2*Δ mutants in Table 2 are consistent with Fra1p and Tsa2p acting together to limit transcription of the iron regulon at the level of Aft1p import into the nucleus (Fig. 6*B*). The mechanism of this inhibition might be the same as that of negative regulation by Fra1p-Tsa1p (30) but would be inducible by virtue of Tsa2p up-regulation when vacuolar acidification is lost.

Additionally, whereas iron supplementation in the *vma* mutant reduced, but did not fully restore, P_{FIT2}-GFP levels, P_{TSA2}-GFP expression was restored to wild-type levels. Collectively, these data suggest an intriguing "braking" system operating in the *vma* mutant. Aft1p-mediated expression of the iron regulon satisfies the iron deprivation signal in the *vma2*Δ mutant, but the mutant may simultaneously overexpress Tsa2p as a protective mechanism, aimed at minimizing iron toxicity while still permitting high affinity iron import.

Previous work has suggested that thioredoxin peroxidases possess functions other than peroxidase activity because they are catalytically inefficient compared with catalases and glutathione peroxidases and are inactivated during H_2O_2 detoxification (60). Although Tsa1p has been shown to act as a molecular chaperone that facilitates protein folding, less is known about the range of functions of Tsa2p. Interestingly, our data suggest new connections to iron and pH homeostasis. Increased Aft1p-GFP translocation in the nucleus (Fig. 6) and induced transcription of the iron regulon (Table 2) in *vma2*Δ*tsa2*Δ double mutants suggest that Tsa2p may function as a negative regulator of Aft1p, possibly in complex with Fra1p. A comparable reduction of transcription from the *FIT2* promoter in *tsa2*Δ*vma2*Δ cells expressing wild-type *TSA2* or the C47S point mutation (Table 2) suggested that Tsa2p is able to limit Aft1p-mediated transcription in a redox-independent manner. The mechanism of this negative regulation by Tsa2p is unclear. Altogether, these data propose a novel function for Tsa2p as a negative regulator of Aft1p upon loss of V-ATPase activity.

Several peroxiredoxins have activities that extend beyond peroxide reduction to include transcriptional regulation (61). The thiol peroxidases, Gpx3p and Ahp1p, bind and regulate activities of the Yap1p and Cad1p transcription factors (62, 63). Furthermore, recent work in *Schizosaccharomyces pombe* showed that the monothiol glutaredoxin, Grx4p, associates with and inhibits the activity of the iron-regulatory proteins Php2 and Fep1 in an iron-dependent manner (64, 65). Several peroxiredoxin homologues exist in most eukaryotes, and the preferential effect of Tsa2p on Aft1p activity establishes a novel function for a protein whose peroxidase activity in the cell is quite redundant. Further work is required to decipher the detailed mechanism by which Tsa2p inhibits Aft1p nuclear localization and/or transcriptional activity.

Acknowledgment—We thank Dr. Jerry Kaplan (University of Utah) for the generous gift of anti-Fra1 antibody.

REFERENCES

1. Bali, P. K., and Aisen, P. (1992) Receptor-induced switch in site-site cooperativity during iron release by transferrin. *Biochemistry* **31,** 3963–3967
2. Cipriano, D. J., Wang, Y., Bond, S., Hinton, A., Jefferies, K. C., Qi, J., and Forgac, M. (2008) Structure and regulation of the vacuolar ATPases. *Biochim. Biophys. Acta* **1777,** 599–604
3. Dautry-Varsat, A., Ciechanover, A., and Lodish, H. F. (1983) pH and the recycling of transferrin during receptor-mediated endocytosis. *Proc. Natl. Acad. Sci. U.S.A.* **80,** 2258–2262
4. Sorkin, A., and Von Zastrow, M. (2002) Signal transduction and endocytosis. Close encounters of many kinds. *Nat. Rev. Mol. Cell Biol.* **3,** 600–614
5. Karmazyn, M., Gan, X. T., Humphreys, R. A., Yoshida, H., and Kusumoto, K. (1999) The myocardial Na^+-H^+ exchange. Structure, regulation, and its role in heart disease. *Circ. Res.* **85,** 777–786
6. Kinouchi, K., Ichihara, A., Sano, M., Sun-Wada, G. H., Wada, Y., Kurauchi-Mito, A., Bokuda, K., Narita, T., Oshima, Y., Sakoda, M., Tamai, Y., Sato, H., Fukuda, K., and Itoh, H. (2010) The (pro)renin receptor/ATP6AP2 is essential for vacuolar H^+-ATPase assembly in murine cardiomyocytes. *Circ. Res.* **107,** 30–34
7. Williamson, W. R., and Hiesinger, P. R. (2010) On the role of v-ATPase V0a1-dependent degradation in Alzheimer disease. *Commun. Integr. Biol.* **3,** 604–607
8. Williamson, W. R., Wang, D., Haberman, A. S., and Hiesinger, P. R. (2010) A dual function of V0-ATPase a1 provides an endolysosomal degradation mechanism in *Drosophila melanogaster* photoreceptors. *J. Cell Biol.* **189,** 885–899
9. Kane, P. M. (2006) The where, when, and how of organelle acidification by the yeast vacuolar H^+-ATPase. *Microbiol. Mol. Biol. Rev.* **70,** 177–191
10. Nishi, T., and Forgac, M. (2002) The vacuolar (H^+)-ATPases. Nature's most versatile proton pumps. *Nat. Rev. Mol. Cell Biol.* **3,** 94–103
11. Breton, S., and Brown, D. (2007) New insights into the regulation of V-ATPase-dependent proton secretion. *Am. J. Physiol. Renal Physiol.* **292,** F1–F10
12. Allan, A. K., Du, J., Davies, S. A., and Dow, J. A. (2005) Genome-wide survey of V-ATPase genes in *Drosophila* reveals a conserved renal phenotype for lethal alleles. *Physiol. Genomics* **22,** 128–138
13. Sun-Wada, G., Murata, Y., Yamamoto, A., Kanazawa, H., Wada, Y., and Futai, M. (2000) Acidic endomembrane organelles are required for mouse postimplantation development. *Dev. Biol.* **228,** 315–325
14. Martínez-Muñoz, G. A., and Kane, P. (2008) Vacuolar and plasma membrane proton pumps collaborate to achieve cytosolic pH homeostasis in yeast. *J. Biol. Chem.* **283,** 20309–20319
15. Tarsio, M., Zheng, H., Smardon, A. M., Martínez-Muñoz, G. A., and Kane, P. M. (2011) Consequences of loss of Vph1 protein-containing vacuolar ATPases (V-ATPases) for overall cellular pH homeostasis. *J. Biol. Chem.* **286,** 28089–28096
16. Bañuelos, M. A., Sychrová, H., Bleykasten-Grosshans, C., Souciet, J. L., and Potier, S. (1998) The Nha1 antiporter of *Saccharomyces cerevisiae* mediates sodium and potassium efflux. *Microbiology* **144,** 2749–2758
17. Pardo, J. M., Cubero, B., Leidi, E. O., and Quintero, F. J. (2006) Alkali cation exchangers. Roles in cellular homeostasis and stress tolerance. *J. Exp. Bot.* **57,** 1181–1199
18. Beauvoit, B., Rigoulet, M., Raffard, G., Canioni, P., and Guérin, B. (1991) Differential sensitivity of the cellular compartments of *Saccharomyces cerevisiae* to protonophoric uncoupler under fermentative and respiratory energy supply. *Biochemistry* **30,** 11212–11220
19. Freimoser, F. M., Hürlimann, H. C., Jakob, C. A., Werner, T. P., and Amrhein, N. (2006) Systematic screening of polyphosphate (poly P) levels in yeast mutant cells reveals strong interdependence with primary metabolism. *Genome Biol.* **7,** R109
20. Milgrom, E., Diab, H., Middleton, F., and Kane, P. M. (2007) Loss of vacuolar proton-translocating ATPase activity in yeast results in chronic oxidative stress. *J. Biol. Chem.* **282,** 7125–7136
21. Jamieson, D. J. (1998) Oxidative stress responses of the yeast *Saccharomyces cerevisiae*. *Yeast* **14,** 1511–1527
22. Brombacher, K., Fischer, B. B., Rüfenacht, K., and Eggen, R. I. (2006) The role of Yap1p and Skn7p-mediated oxidative stress response in the defence of *Saccharomyces cerevisiae* against singlet oxygen. *Yeast* **23,** 741–750
23. Thorpe, G. W., Fong, C. S., Alic, N., Higgins, V. J., and Dawes, I. W. (2004) Cells have distinct mechanisms to maintain protection against different reactive oxygen species. Oxidative-stress-response genes. *Proc. Natl. Acad. Sci. U.S.A.* **101,** 6564–6569
24. Berggren, M. I., Husbeck, B., Samulitis, B., Baker, A. F., Gallegos, A., and Powis, G. (2001) Thioredoxin peroxidase-1 (peroxiredoxin-1) is increased in thioredoxin-1 transfected cells and results in enhanced protection against apoptosis caused by hydrogen peroxide but not by other agents including dexamethasone, etoposide, and doxorubicin. *Arch. Biochem. Biophys.* **392,** 103–109
25. Wong, C. M., Zhou, Y., Ng, R. W., Kung Hf, H. F., and Jin, D. Y. (2002) Cooperation of yeast peroxiredoxins Tsa1p and Tsa2p in the cellular defense against oxidative and nitrosative stress. *J. Biol. Chem.* **277,** 5385–5394
26. Munhoz, D. C., and Netto, L. E. (2004) Cytosolic thioredoxin peroxidase I and II are important defenses of yeast against organic hydroperoxide insult. Catalases and peroxiredoxins cooperate in the decomposition of H_2O_2 by yeast. *J. Biol. Chem.* **279,** 35219–35227
27. Iraqui, I., Kienda, G., Soeur, J., Faye, G., Baldacci, G., Kolodner, R. D., and Huang, M. E. (2009) Peroxiredoxin Tsa1 is the key peroxidase suppressing genome instability and protecting against cell death in *Saccharomyces cerevisiae*. *PLoS Genet.* **5,** e1000524
28. Sideri, T. C., Stojanovski, K., Tuite, M. F., and Grant, C. M. (2010) Ribosome-associated peroxiredoxins suppress oxidative stress-induced *de novo* formation of the [PSI^+] prion in yeast. *Proc. Natl. Acad. Sci. U.S.A.* **107,** 6394–6399
29. Trotter, E. W., Rand, J. D., Vickerstaff, J., and Grant, C. M. (2008) The yeast Tsa1 peroxiredoxin is a ribosome-associated antioxidant. *Biochem. J.* **412,** 73–80
30. Li, L., Murdock, G., Bagley, D., Jia, X., Ward, D. M., and Kaplan, J. (2010) Genetic dissection of a mitochondria-vacuole signaling pathway in yeast reveals a link between chronic oxidative stress and vacuolar iron transport. *J. Biol. Chem.* **285,** 10232–10242
31. Philpott, C. C., and Protchenko, O. (2008) Response to iron deprivation in *Saccharomyces cerevisiae*. *Eukaryot. Cell* **7,** 20–27
32. Courel, M., Lallet, S., Camadro, J. M., and Blaiseau, P. L. (2005) Direct activation of genes involved in intracellular iron use by the yeast iron-responsive transcription factor Aft2 without its paralog Aft1. *Mol. Cell Biol.* **25,** 6760–6771
33. Yamaguchi-Iwai, Y., Ueta, R., Fukunaka, A., and Sasaki, R. (2002) Subcellular localization of Aft1 transcription factor responds to iron status in *Saccharomyces cerevisiae*. *J. Biol. Chem.* **277,** 18914–18918
34. Rutherford, J. C., Ojeda, L., Balk, J., Mühlenhoff, U., Lill, R., and Winge, D. R. (2005) Activation of the iron regulon by the yeast Aft1/Aft2 transcription factors depends on mitochondrial but not cytosolic iron-sulfur

protein biogenesis. *J. Biol. Chem.* **280,** 10135–10140
35. Kumánovics, A., Chen, O. S., Li, L., Bagley, D., Adkins, E. M., Lin, H., Dingra, N. N., Outten, C. E., Keller, G., Winge, D., Ward, D. M., and Kaplan, J. (2008) Identification of FRA1 and FRA2 as genes involved in regulating the yeast iron regulon in response to decreased mitochondrial iron-sulfur cluster synthesis. *J. Biol. Chem.* **283,** 10276–10286
36. Li, H., Mapolelo, D. T., Dingra, N. N., Naik, S. G., Lees, N. S., Hoffman, B. M., Riggs-Gelasco, P. J., Huynh, B. H., Johnson, M. K., and Outten, C. E. (2009) The yeast iron regulatory proteins Grx3/4 and Fra2 form heterodimeric complexes containing a [2Fe-2S] cluster with cysteinyl and histidyl ligation. *Biochemistry* **48,** 9569–9581
37. Valko, M., Morris, H., and Cronin, M. T. (2005) Metals, toxicity and oxidative stress. *Curr. Med. Chem.* **12,** 1161–1208
38. Tong, A. H., Evangelista, M., Parsons, A. B., Xu, H., Bader, G. D., Pagé, N., Robinson, M., Raghibizadeh, S., Hogue, C. W., Bussey, H., Andrews, B., Tyers, M., and Boone, C. (2001) Systematic genetic analysis with ordered arrays of yeast deletion mutants. *Science* **294,** 2364–2368
39. Longtine, M. S., McKenzie, A., 3rd, Demarini, D. J., Shah, N. G., Wach, A., Brachat, A., Philippsen, P., and Pringle, J. R. (1998) Additional modules for versatile and economical PCR-based gene deletion and modification in *Saccharomyces cerevisiae*. *Yeast* **14,** 953–961
40. Kane, P. M., Kuehn, M. C., Howald-Stevenson, I., and Stevens, T. H. (1992) Assembly and targeting of peripheral and integral membrane subunits of the yeast vacuolar H^+-ATPase. *J. Biol. Chem.* **267,** 447–454
41. Pierik, A. J., Netz, D. J., and Lill, R. (2009) Analysis of iron-sulfur protein maturation in eukaryotes. *Nat. Protoc.* **4,** 753–766
42. Ghaemmaghami, S., Huh, W. K., Bower, K., Howson, R. W., Belle, A., Dephoure, N., O'Shea, E. K., and Weissman, J. S. (2003) Global analysis of protein expression in yeast. *Nature* **425,** 737–741
43. Urbanowski, J. L., and Piper, R. C. (1999) The iron transporter Fth1p forms a complex with the Fet5 iron oxidase and resides on the vacuolar membrane. *J. Biol. Chem.* **274,** 38061–38070
44. Ojeda, L., Keller, G., Muhlenhoff, U., Rutherford, J. C., Lill, R., and Winge, D. R. (2006) Role of glutaredoxin-3 and glutaredoxin-4 in the iron regulation of the Aft1 transcriptional activator in *Saccharomyces cerevisiae*. *J. Biol. Chem.* **281,** 17661–17669
45. Chen, O. S., Crisp, R. J., Valachovic, M., Bard, M., Winge, D. R., and Kaplan, J. (2004) Transcription of the yeast iron regulon does not respond directly to iron but rather to iron-sulfur cluster biosynthesis. *J. Biol. Chem.* **279,** 29513–29518
46. Pujol-Carrion, N., Belli, G., Herrero, E., Nogues, A., and de la Torre-Ruiz, M. A. (2006) Glutaredoxins Grx3 and Grx4 regulate nuclear localisation of Aft1 and the oxidative stress response in *Saccharomyces cerevisiae*. *J. Cell Sci.* **119,** 4554–4564
47. Li, H., Mapolelo, D. T., Dingra, N. N., Keller, G., Riggs-Gelasco, P. J., Winge, D. R., Johnson, M. K., and Outten, C. E. (2011) Histidine 103 in Fra2 is an iron-sulfur cluster ligand in the [2Fe-2S] Fra2-Grx3 complex and is required for *in vivo* iron signaling in yeast. *J. Biol. Chem.* **286,** 867–876
48. Irazusta, V., Moreno-Cermeño, A., Cabiscol, E., Ros, J., and Tamarit, J. (2008) Major targets of iron-induced protein oxidative damage in frataxin-deficient yeasts are magnesium-binding proteins. *Free Radic. Biol. Med.* **44,** 1712–1723
49. Wong, C. M., Ching, Y. P., Zhou, Y., Kung, H. F., and Jin, D. Y. (2003) Transcriptional regulation of yeast peroxiredoxin gene TSA2 through Hap1p, Rox1p, and Hap2/3/5p. *Free Radic. Biol. Med.* **34,** 585–597
50. Herrero, E., Ros, J., Bellí, G., and Cabiscol, E. (2008) Redox control and oxidative stress in yeast cells. *Biochim. Biophys. Acta* **1780,** 1217–1235
51. Follmann, M., Ochrombel, I., Krämer, R., Trötschel, C., Poetsch, A., Rückert, C., Hüser, A., Persicke, M., Seiferling, D., Kalinowski, J., and Marin, K. (2009) Functional genomics of pH homeostasis in *Corynebacterium glutamicum* revealed novel links between pH response, oxidative stress, iron homeostasis and methionine synthesis. *BMC Genomics* **10,** 621
52. Cockrell, A. L., Holmes-Hampton, G. P., McCormick, S. P., Chakrabarti, M., and Lindahl, P. A. (2011) Mossbauer and EPR study of iron in vacuoles from fermenting *Saccharomyces cerevisiae*. *Biochemistry* **50,** 10275–10283
53. Davis-Kaplan, S. R., Ward, D. M., Shiflett, S. L., and Kaplan, J. (2004) Genome-wide analysis of iron-dependent growth reveals a novel yeast gene required for vacuolar acidification. *J. Biol. Chem.* **279,** 4322–4329
54. Rand, J. D., and Grant, C. M. (2006) The thioredoxin system protects ribosomes against stress-induced aggregation. *Mol. Biol. Cell* **17,** 387–401
55. Jang, H. H., Lee, K. O., Chi, Y. H., Jung, B. G., Park, S. K., Park, J. H., Lee, J. R., Lee, S. S., Moon, J. C., Yun, J. W., Choi, Y. O., Kim, W. Y., Kang, J. S., Cheong, G. W., Yun, D. J., Rhee, S. G., Cho, M. J., and Lee, S. Y. (2004) Two enzymes in one. Two yeast peroxiredoxins display oxidative stress-dependent switching from a peroxidase to a molecular chaperone function. *Cell* **117,** 625–635
56. Serrano, R., Bernal, D., Simón, E., and Ariño, J. (2004) Copper and iron are the limiting factors for growth of the yeast *Saccharomyces cerevisiae* in an alkaline environment. *J. Biol. Chem.* **279,** 19698–19704
57. Davis-Kaplan, S. R., Askwith, C. C., Bengtzen, A. C., Radisky, D., and Kaplan, J. (1998) Chloride is an allosteric effector of copper assembly for the yeast multicopper oxidase Fet3p. An unexpected role for intracellular chloride channels. *Proc. Natl. Acad. Sci. U.S.A.* **95,** 13641–13645
58. Spizzo, T., Byersdorfer, C., Duesterhoeft, S., and Eide, D. (1997) The yeast FET5 gene encodes a FET3-related multicopper oxidase implicated in iron transport. *Mol. Gen. Genet.* **256,** 547–556
59. Hirsch, J., Marin, E., Floriani, M., Chiarenza, S., Richaud, P., Nussaume, L., and Thibaud, M. C. (2006) Phosphate deficiency promotes modification of iron distribution in *Arabidopsis* plants. *Biochimie* **88,** 1767–1771
60. Yang, K. S., Kang, S. W., Woo, H. A., Hwang, S. C., Chae, H. Z., Kim, K., and Rhee, S. G. (2002) Inactivation of human peroxiredoxin I during catalysis as the result of the oxidation of the catalytic site cysteine to cysteine-sulfinic acid. *J. Biol. Chem.* **277,** 38029–38036
61. Fomenko, D. E., Koc, A., Agisheva, N., Jacobsen, M., Kaya, A., Malinouski, M., Rutherford, J. C., Siu, K. L., Jin, D. Y., Winge, D. R., and Gladyshev, V. N. (2011) Thiol peroxidases mediate specific genome-wide regulation of gene expression in response to hydrogen peroxide. *Proc. Natl. Acad. Sci. U.S.A.* **108,** 2729–2734
62. Delaunay, A., Pflieger, D., Barrault, M. B., Vinh, J., and Toledano, M. B. (2002) A thiol peroxidase is an H_2O_2 receptor and redox-transducer in gene activation. *Cell* **111,** 471–481
63. Iwai, K., Naganuma, A., and Kuge, S. (2010) Peroxiredoxin Ahp1 acts as a receptor for alkylhydroperoxides to induce disulfide bond formation in the Cad1 transcription factor. *J. Biol. Chem.* **285,** 10597–10604
64. Jbel, M., Mercier, A., and Labbé, S. (2011) Grx4 monothiol glutaredoxin is required for iron limitation-dependent inhibition of Fep1. *Eukaryot. Cell* **10,** 629–645
65. Vachon, P., Mercier, A., Jbel, M., and Labbé, S. (2012) The monothiol glutaredoxin Grx4 exerts an iron-dependent inhibitory effect on Php4 function. *Eukaryot. Cell* **11,** 806–819